

Experimental Evidence for the Aggregation of [(Phen)₂Pd₂(μ-H)(μ-CO)]⁺ in Solution

Alceo Macchioni,* Aldo Romani, and Cristiano Zuccaccia

Dipartimento di Chimica, Università degli Studi di Perugia, Via Elce di Sotto 8,
06123 Perugia, Italy

Gianfranco Guglielmetti and Cecilia Querci

Polimeri Europa S. p. A., Istituto Guido Donegani, Via Fauser 4, 28100 Novara, Italy

Received December 2, 2002

The aggregation in solution of the dinuclear palladium(I) complex [(Phen)₂Pd₂(μ-H)(μ-CO)]⁺BARF₄⁻ (**1c**) was investigated by PGSE NMR, UV–vis, and ESI- and FAB-mass techniques. PGSE measurements showed that only the cationic moiety of **1c** (**1c**⁺) is involved in the aggregation process, while the counteranion does not participate in it. By using compound [Pd(Phen)(Me)Cl] (**2**) as an external standard, it was found that, depending on the solution concentration, the volume ratio V_{1c^+}/V_2 ranges from 7.2 to 40.2 in nitrobenzene-*d*₅ at 296 K. The V_{1c^+}/V_2 value (ca. 5.5) extrapolated to infinite dilution indicates that, even at very low concentration values, at least two units of **1c**⁺ are associated to form a dimer. At the highest possible concentration (55.20 mM) a mean aggregate bearing about 20 **1c**⁺ units is present in solution, having an average hydrodynamic radius of 11–12 Å. The dependence of the ¹H NMR chemical shifts (for acetone-*d*₆ or nitrobenzene-*d*₅ solutions at 296 K) and UV–vis spectra (in THF or nitrobenzene at 296 K) on the concentration and of the UV–vis spectra on the temperature (from 323 to 153 K) indicates that two different aggregation processes are present, having well differentiated interaction energies. Although the latter were not quantitatively evaluated, the experimental results indicate that the interaction energy of the process occurring at low concentration (responsible for the dimer formation) is much larger than that relative to the formation of higher aggregates. As a confirmation, ESI- and FAB-mass results show the presence of peaks related to the fragmentation of the dimeric species containing four palladium atoms, indicating that such a dimer has remarkable stability.

Introduction

Noncovalent interactions¹ greatly affect the structure and reactivity of transition-metal complexes.² They are often responsible for the formation of adducts with variable nuclearity in which the noncovalently bonded moieties specifically interact.

Since 1996³ we have been applying NMR methodologies to investigate metallorganic noncovalent adducts (mainly ion pairs) in solution with the principal aim of correlating their structural features with the stoichiometric and catalytic reactivity. In particular, NOE (nuclear Overhauser effect) NMR spectroscopy⁴ was used to obtain information about the relative orientation

of the noncovalently bonded units,⁵ while PGSE (pulsed-field gradient spin–echo) NMR experiments⁶ afforded specific information on the aggregate nuclearity in solution, in that the hydrodynamic radii and the volumes of the diffusing particles could be estimated.⁷

In this paper we report the results of applying the latter methodology, combined with those from UV–vis

* To whom correspondence should be addressed. E-mail: alceo@unipg.it.

(1) Müller-Dethlefs, K.; Hobza, P. *Chem. Rev.* **2000**, *100*, 143. Williams, D. H.; Westwell, M. S. *Chem. Soc. Rev.* **1998**, *27*, 57. Israelachvili, J. *Intermolecular & Surface Forces*; Academic Press: London, 1992.

(2) Landau, S. E.; Groh, K. E.; Lough, A. J.; Morris, R. H. *Inorg. Chem.* **2002**, *41*, 2995. Gruet, K.; Clot, E.; Eisenstein, O.; Lee, D. H.; Patel, B.; Macchioni, A.; Crabtree, R. H. *New. J. Chem.* **2003**, *27*, 80. Chen, E. Y.-X.; Marks, T. J. *Chem. Rev.* **2000**, *100*, 1391. Ittel, S. D.; Johnson, L. K.; Brookhart, M. *Chem. Rev.* **2000**, *100*, 1169. Evans, D. A.; Murry, J. A.; von Matt, P.; Norcross, R. D.; Miller, S. J. *Angew. Chem., Int. Ed. Engl.* **1995**, *34*, 798. Kündig, E. P.; Saudan, C. M.; Bernardinelli, G. *Angew. Chem., Int. Ed.* **1999**, *38*, 1220.

(3) Bellachioma, G.; Cardaci, G.; Macchioni, A.; Reichenbach, G.; Terenzi, S. *Organometallics* **1996**, *15*, 4349.

(4) Neuhaus, D.; Williamson, M. *The Nuclear Overhauser Effect in Structural and Conformational Analysis*; Wiley-VCH: Weinheim, Germany, 2000.

(5) For recent references see: Macchioni, A. *Eur. J. Inorg. Chem.* **2003**, 195. Binotti, B.; Bellachioma, G.; Cardaci, G.; Macchioni, A.; Zuccaccia, C.; Foresti, E.; Sabatino, P. *Organometallics* **2002**, *21*, 346. Zuccaccia, C.; Bellachioma, G.; Cardaci, G.; Macchioni, A. *J. Am. Chem. Soc.* **2001**, *123*, 11020. Macchioni, A.; Zuccaccia, C.; Clot, E.; Gruet, K.; Crabtree, R. H. *Organometallics* **2001**, *20*, 2367.

(6) Johnson, C. S., Jr. *Prog. Nucl. Magn. Reson. Spectrosc.* **1999**, *34*, 203. Price, W. S. *Concepts Magn. Reson.* **1997**, *9*, 299. Price, W. S. *Concepts Magn. Reson.* **1998**, *10*, 197. Stilbs, P. *Prog. Nucl. Magn. Reson. Spectrosc.* **1987**, *19*, 1. Stejskal, E. O.; Tanner, J. E. *J. Chem. Phys.* **1965**, *42*, 288.

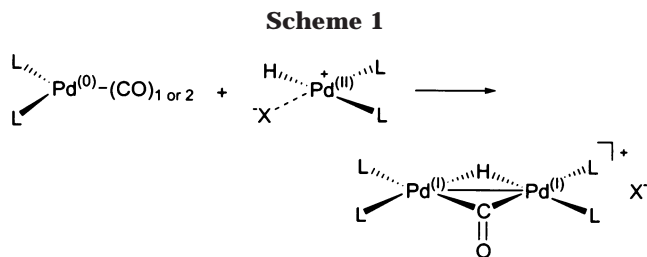
(7) For some recent references see: Babushkin, D. E.; Brintzinger, H. H. *J. Am. Chem. Soc.* **2002**, *124*, 12869. Burini, A.; Fackler, J. P., Jr.; Galassi, R.; Macchioni, A.; Omary, M. A.; Rawashdeh-Omary, M. A.; Pietroni, B. R.; Sabatini, S.; Zuccaccia, C. *J. Am. Chem. Soc.* **2002**, *124*, 4570. Drago, D.; Pregosin, P. S.; Pfaltz, A. *Chem. Commun.* **2002**, 286. Valentini, M.; Rügger, H.; Pregosin, P. S. *Helv. Chim. Acta* **2001**, *84*, 2833. Zuccaccia, C.; Bellachioma, G.; Cardaci, G.; Macchioni, A. *Organometallics* **2000**, *19*, 4663. Valentini, M.; Rügger, H.; Pregosin, P. S. *Organometallics* **2000**, *19*, 2551. Beck, S.; Geyer, A.; Brintzinger, H. H. *Chem. Commun.* **1999**, 2477. Olenyuk, B.; Lovin, M. D.; Whiteford, J. A.; Stang, P. J. *J. Am. Chem. Soc.* **1999**, *121*, 10434–10435.

spectroscopy and ESI- and FAB-mass spectrometry studies, to investigate the aggregation in solution of the cationic dinuclear Pd(I) compound $[(\text{Phen})_2\text{Pd}_2(\mu\text{-H})(\mu\text{-CO})]^+\text{X}^-$ (**1**), bearing H- and CO-bridging ligands (Phen = 1,10-phenanthroline). In general, dinuclear $[(\text{L}_2\text{Pd})_2(\mu\text{-H})(\mu\text{-CO})]\text{X}$ compounds were observed during several carbonylation reactions as byproducts having little catalytic activity.⁸ In the cases in which $\text{L}_2 = 2 \text{ PR}_3$ or P,P ligands, they were completely characterized both in the solid state and in solution and their reactivity was studied in depth.^{8a-c} In contrast, very little is known about $\text{L}_2 = \text{N,N}$ ligands, because the compounds are usually insoluble in most of the usual solvents and are completely amorphous. To the best of our knowledge, only Wong et al.⁹ were able to obtain crystals suitable for an X-ray investigation of this class of compounds. In particular, the solid-state structure was solved for $[(\text{Bipy})_2\text{Pd}_2(\mu\text{-H})(\mu\text{-CO})][\text{H}_3\text{Os}_4(\text{CO})_{12}]$ (Bipy = 2,2'-bipyridine) and it was shown that the bipyridine moieties of the cationic moieties stack in the solid state with the cations aligned in a paired manner, while the consecutive cations lay in opposite directions with respect to the bridging carbonyl. Due to the fact that compounds **1** were found to be the byproduct of the synthesis of hydrogen peroxide from carbon monoxide, water, and oxygen¹⁰ and that they formed from the reaction of the catalysts for the CO/styrene copolymerization, $[\text{Pd}(\eta^1\text{-}\eta^2\text{-C}_8\text{H}_{12}\text{OMe})(\text{N,N})]\text{X}$,¹¹ with carbon monoxide, we decided to undertake a detailed study of its behavior in solution. In particular, special attention was given to the possibility that compounds **1** could aggregate in solution as a consequence of aromatic π -stacking.¹² The results of this study are now reported.

Results and Discussion

Synthesis of Complexes 1a–c. The complex $[(\text{Phen})_2\text{Pd}_2(\mu\text{-H})(\mu\text{-CO})]\text{CH}_3\text{COO}$ (**1a**) forms as a byproduct during the synthesis of hydrogen peroxide from carbon monoxide, water, and oxygen catalyzed by a palladium catalyst.¹⁰ Complex **1a** was consequently prepared with this procedure by the reaction of $\text{Pd}(\text{phen})(\text{CH}_3\text{COO})_2$ with CO in a biphasic medium (toluene and 1-butanol/ H_2O) acidified with CH_3COOH . From literature studies carried out on analogous compounds with P- instead of N-ligands,^{8a-c} it seems that the dinuclear palladium(I) compounds, bearing H and CO bridges, form from the combination of $\text{PdH}(\text{CH}_3\text{COO})(\text{L})_2$ and $\text{Pd}(\text{CO})(\text{L})_2$, as illustrated in Scheme 1.

Complex **1a** is a red amorphous solid insoluble in most of the usual solvents. It dissolves very little in methanol, nitromethane, and DMSO, where it slowly decomposes. Complex **1b**, having PF_6^- as a counteranion, could be



prepared by suspending **1a** in methanol containing $\text{NH}_4\text{-PF}_6$. $\text{NH}_4\text{CH}_3\text{COOH}$ formed in solution, while the anion metathesis occurred in the solid state. Complex **1b** presents the same solubility problems as **1a**, but it is much more stable in solution. Progress was made in the solubility feature by preparing complex **1c** bearing the BAR_4^- counteranion ($\text{BAR}_4^- = \text{B}[3,5\text{-(CF}_3)_2\text{-C}_6\text{H}_3]_4^-$) by the reaction of **1a** or **1b** with NaBAR_4 in methanol followed by the precipitation of **1c** as a consequence of adding water. Complexes **1b,c** are also completely amorphous, and all our attempts to obtain single crystals for X-ray studies were unsuccessful. Furthermore, their red powders were analyzed with a X-ray diffractometer for powders, and no indication of microcrystallinity was found.

Intramolecular Characterization. The NMR characterization of complexes **1** was carried out in acetone- d_6 (296 K, 9×10^{-2} M), THF- d_8 (273 K), and nitrobenzene- d_5 (296 K) by ^1H , ^{13}C , ^{19}F , $^1\text{H-COSY}$, $^1\text{H-NOESY}$, ^{19}F , $^1\text{H-HOESY}$, $^1\text{H},^{13}\text{C}$ HMQC NMR, and $^1\text{H},^{13}\text{C}$ HMBC NMR spectroscopy. Since we did not observe any significant difference in the characterization parameters of the cationic moiety of **1a–c** and since complex **1c** was used for the PGSE NMR experiments, we will only consider the latter complex. In addition to the typical sets of the phenanthroline ligand having different ligands in trans positions, the ^1H and ^{13}C NMR spectra showed one ^1H resonance at -14.60 ppm and one carbonyl resonance at 226.2 ppm. The areas of such resonances were half of those relative to phenanthroline protons or carbons. These observations alone strongly suggested that compounds **1** contained two “Pd(Phen)” units held together by H and CO bridging ligands. The starting point for assigning the resonances was based on the observation of a NOE interaction between the hydride and an aromatic proton at 8.91 ppm that was, consequently, assigned to H9 (for numbering see Chart 1). All the other aromatic protons were identified by combining the information from the scalar and dipolar connectivities in the $^1\text{H-COSY}$ and the $^1\text{H-NOESY}$ spectra, respectively.

The assignment of the nonquaternary carbon resonances was obtained straightaway by the indirect $^1\text{H},^{13}\text{C}$

(8) (a) Moshe, P.; Milstein, D. *Organometallics* **1994**, *13*, 600–609. (b) Toth, I.; Elsevier, C. J. *Organometallics* **1994**, *13*, 2118–2122. (c) Sperrle, M.; Gramlich, V.; Consiglio, G. *Organometallics* **1995**, *15*, 5196–5201. (d) Bianchini, C.; Meli, A. *Coord. Chem. Rev.* **2002**, *225*, 35. (e) For a review on hydrido complexes of palladium see: Grushin, V. V. *Chem. Rev.* **1996**, *96*, 2011.

(9) Chan, S.; Lee, S.-M.; Lin, Z.; Wong, W.-T. *J. Organomet. Chem.* **1996**, *510*, 219.

(10) Bianchi, D.; Bartolo, R.; Querci, C.; D'Aloiso, R.; Ricci, M. *Stud. Surf. Sci. Catal.* **2001**, *139*, 327–334. Querci, C.; D'Aloiso, R.; Bortolo, R.; Ricci, M.; Bianchi, D. *J. Mol. Catal. A* **2001**, *176*, 95–100. Bianchi, D.; Bortolo, R.; D'Aloiso, R.; Ricci, M. *Angew. Chem., Int. Ed.* **1999**, *38*, 706–708.

(11) Mestroni, G.; Milani B. Personal communication.

(12) Shetty, A. S.; Zhang, J.; Moore, J. S. *J. Am. Chem. Soc.* **1996**, *118*, 1019 and references therein.

HMQC correlations. The detection of the $^3J_{\text{CH}}$ long-range correlations in the phenanthroline ligand and the $^2J_{\text{CH}}$ value between the carbonylic carbon and the hydride allowed the quaternary carbon to be assigned, also. The value of the latter coupling constant was established by recording a ^{13}C carbon spectrum without decoupling the hydride proton: $^2J_{\text{CH}} = 0.9$ Hz. The assignments of the anion resonances were immediately carried out because they did not differ from the data reported in the literature.¹³ The correspondence between the compound present in solution with that in the solid state was checked by recording a CP MAS ^{13}C NMR spectrum for complex **1a**. The solid-state ^{13}C NMR chemical shift values agreed perfectly with those found in solution.

A comparison of the NMR data relative to complexes **1** and those of analogous complexes bearing P-ligands has some interesting features. In the latter compounds the bridging hydride and carbonyl groups resonate at about -5.0 and $240\text{--}250$ ppm,^{8a-c} respectively, while they resonate at a much lower frequency in **1** (-14.60 and 226.2 ppm). Furthermore, complexes bearing N-ligands are rigid on the chemical shift time scale, while those with P-ligands are dynamic above -10 °C.^{8a-c} These observations can be explained, as mentioned by Wong,⁹ considering that the replacement of π -acid ligands (P) by better σ -donor ligands (N) strengthens the Pd–H and Pd–CO bonds, affording higher shielding of H and CO groups and slowing down the dynamic process in which the two N-arms are exchanged that occurs through the breaking of these bonds.

PGSE NMR Measurements. The measurements were carried out for complex **1c** due to its reasonable solubility in several solvents that allowed the concentration dependence of the self-diffusion coefficients to be investigated and, consequently, the aggregation of the sample concentration. Furthermore, we suspected that only the cationic moiety participated in the aggregation phenomenon. Due to its poorly coordinating tendency, $\text{BAr}^{\text{F}_4^-}$ was the ideal counteranion for carrying out the experiments. This second point also guided the choice of the solvent in that, among the solvents in which **1c** is soluble, we decided to use the one with the highest dielectric constant (nitrobenzene- d_5 , $\epsilon = 34.82$, $T = 298$ K). To be sure that $\text{BAr}^{\text{F}_4^-}$ did not participate in the aggregation phenomena, several ^{19}F , ^1H -HOESY and ^1H -NOESY NMR spectra were recorded for complex **1c** in THF- d_8 ($\epsilon = 7.58$, $T = 298$ K), acetone- d_6 ($\epsilon = 20.7$, $T = 298$ K), and nitrobenzene- d_5 . No interionic NOEs were observed. This indicates that even in THF intimate ion pairs are not significantly present.⁵

The PGSE NMR measurements were performed by using the standard stimulated echo pulse sequence^{6,7} at room temperature. The dependence of the resonance intensity (I) on a constant waiting time and on a varied gradient strength (G) is described by eq 1, where $I =$

$$\ln \frac{I}{I_0} = -(\gamma\delta)^2 D \left(\Delta - \frac{\delta}{3} \right) G^2 \quad (1)$$

intensity of the observed spin-echo, $I_0 =$ intensity of the spin-echo without gradients, $D =$ diffusion coef-

ficient, $\Delta =$ delay between the midpoints of the gradients, $\delta =$ length of the gradient pulse, and $\gamma =$ magnetogyric ratio. The diffusion coefficient D is directly proportional to the slope of the regression line ($-m$) divided by $\Delta - \delta/3$. According to the Stokes–Einstein equation (eq 2), the diffusion coefficient is proportional

$$D_t = \frac{kT}{6\pi\eta r_H} \quad (2)$$

to $1/r_H$ (where r_H represents the hydrodynamic radius of the diffusing particle). k is the Boltzmann constant, T is the absolute temperature, and η is the viscosity. Consequently, D^3 is inversely proportional to the volume (V) of the diffusing particle that in the Stokes–Einstein model is assumed to be spherical. As shown in eq 2, D is also inversely proportional to the solution viscosity that must be taken into account if the D , r_H , or V values between solutions having different solvents or concentrations are to be compared.

In this case we were interested in the aggregation of complex **1c** in a particular solvent as a function of the solution concentration. To obtain information independent of the solution viscosity, we decided to measure the diffusion coefficients for **1c** relative to those of $[\text{Pd}(\text{Phen})(\text{Me})\text{Cl}]$ (**2**). Complex **2** can be considered a good standard for **1c**, because their shapes are similar. In addition, its volume can reasonably be considered to be half that of the cationic moiety of **1c** ($\mathbf{1c}^+$) and, consequently, from the ratio of the volume of $\mathbf{1c}^+$ and that of **2** multiplied by 2, an idea about the presence and the entity of aggregation is immediately obtained. On the other hand, we soon realized that it was not possible to use complex **2** as an internal standard because it participated in the aggregation of $\mathbf{1c}^+$ as the concentration increased (Supporting Information). For this reason, we decided to add tetramethylsilane (TMS) as internal standard in the solutions of $\mathbf{1c}^+$ at different concentrations and to perform a measurement of a dilute solution of **2** and TMS. Because TMS does not participate in the aggregation of **1c**, the difference observed in the D values in the $\mathbf{1c}^+$ solutions and in the reference solution with **2** must be due only to a change in viscosity. When the ratio $D_{\mathbf{1c}^+}/D_{\text{TMS}}$ is multiplied by the ratio D_{TMS}/D_2 , a comparison between the diffusion coefficient of $\mathbf{1c}^+$ and that of **2** is obtained which does not depend on the viscosity of the **1c** solutions. In Table 1 we report the data of the PGSE measurements carried out in nitrobenzene- d_5 . The diffusion coefficients decrease as the sample concentration increases, but the decrease for $\mathbf{1c}^+$ is more marked. This is illustrated in Figure 1, where the trends of the TMS and A^- diffusion coefficients (D_{TMS} and D_{A^-} , respectively) are almost linear, indicating that, reasonably, the solution viscosity is linearly dependent on the sample concentration. On the other hand, the decrease of the $\mathbf{1c}^+$ diffusion coefficient ($D_{\mathbf{1c}^+}$) with the concentration is not linear (Figure 1) and, consequently, is due not only to an increased viscosity but also to aggregation phenomena. In Table 1 the ratios $D_{\mathbf{1c}^+}/D_{\text{TMS}}$ and $D_{\text{A}^-}/D_{\text{TMS}}$, which should be independent of the solution viscosity if aggregation phenomena are not present, are also reported. While $D_{\mathbf{1c}^+}/D_{\text{TMS}}$ still decreases with the concentration, $D_{\text{A}^-}/D_{\text{TMS}}$ values seem to be independent of C . This indicates that an aggregation process is present but involves only the cation $\mathbf{1c}^+$.

(13) Macchioni, A.; Bellachioma, G.; Cardaci, G.; Travaglia, M.; Zuccaccia, C.; Milani, B.; Corso, G.; Zangrando, E.; Mestroni, G.; Carfagna, C.; Formica, M. *Organometallics* **1999**, *18*, 3061.

Table 1. Relevant Data for the PGSE NMR Measurements Carried Out in Nitrobenzene- d_5 at 296 K

C_{1c} (mM)	$10^{10}D_{1c^{+a}}$ (m^2s^{-1})	$10^{10}D_{A^{-a}}$ (m^2s^{-1})	$10^{10}D_{\text{TMS}^a}$ (m^2s^{-1})	D_{1c^+}/D_{TMS}	D_{A^-}/D_{TMS}	V_{1c^+}/V_2	V_{A^-}/V_2
0.43 ^b	1.79	2.17	7.40	0.238	0.288	7.2	4.6
1.19	1.69	2.21	7.39	0.229	0.300	9.2	4.1
4.18	1.45	2.10	7.33	0.197	0.286	14.4	4.7
8.06	1.32	1.91	7.22	0.182	0.265	18.2	5.9
13.41	1.21	1.98	7.05	0.172	0.282	21.8	4.9
25.12	1.07	1.87	6.96	0.154	0.268	30.6	5.7
40.31	0.95	1.73	6.46	0.146	0.268	35.2	5.7
55.20	0.86	1.66	6.16	0.140	0.269	40.2	5.7

^a D values were estimated by measuring the $-m/(\Delta - \delta/3)$ parameter for a sample of HDO (5%) in D_2O (known diffusion coefficient $1.902 \times 10^{-9} \text{ m}^2/\text{s}$)²² under the same conditions as those for complex **1c**. In the cases of $1c^+$ and A^- , the D data are the mean of the individual values obtained by the straight-lines for individual NMR signals. The mean deviations for the average values reported here are less than 5%. ^b In the presence of **2** as internal standard (Supporting Information).

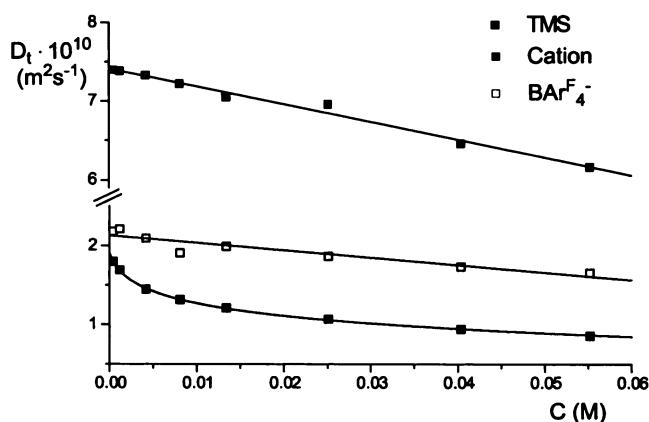


Figure 1. Dependence of the diffusion coefficients (D_i) on the concentration for TMS, the cationic moiety of **1c**, and the BARF_4^- anion. The first two trends show a linear decrement of D_i , while the latter is more marked, indicating the presence of cationic aggregation phenomena.

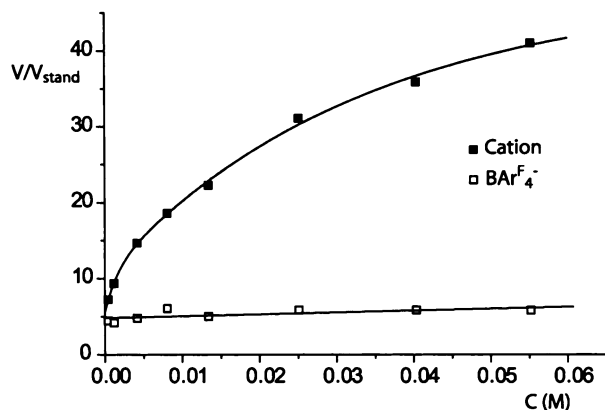


Figure 2. Dependence of the cation and anion volumes relative to that of the **2** standard on the **1c** concentration (C). While the cation volume is strongly affected by C , that of the anion remains practically constant.

As mentioned above, the V_{1c^+}/V_2 and V_{A^-}/V_2 volume ratios can be estimated by multiplying D_{1c^+}/D_{TMS} and D_{A^-}/D_{TMS} by D_2/D_{TMS} and elevating the product to -3 (Table 1). The trends of V_{1c^+}/V_2 and V_{A^-}/V_2 versus C are reported in Figure 2. It can be seen that V_{A^-}/V_2 seems to be independent of C , as anticipated above, and the mean value amounts to 5.2. The V_{A^-}/V_2 theoretical value of 3.8, estimated from X-ray data, is in reasonably good agreement with the experimentally determined mean value, considering that (1) ionic species always drag some solvent molecules during the translation¹⁴ and (2)

Table 2. Aggregate Average Volume and Radius as a Function of the Concentration for Complex 1c

C_{1c} (mM)	V_{1c^+}/V_2	$10^{10}D_{1c^{+c}}$ (m^2s^{-1})	$V_{1c^{+a}}$ (\AA^3)	r_H^a (\AA)	r_H^b (\AA)
0.43	8.2	1.76	1624	7.3	6.4
1.19	9.2	1.69	1821	7.6	6.7
4.18	14.4	1.46	2851	8.8	7.8
8.06	18.2	1.35	3604	9.5	8.4
13.41	21.8	1.27	4316	10.1	8.9
25.12	30.6	1.13	6059	11.3	10.0
40.31	35.2	1.08	6970	11.9	10.5
55.20	40.2	1.03	7960	12.4	11.0

^a The aggregate volumes (V_{1c^+}) were calculated from the theoretical volume of **2** (198 \AA^3) determined from X-ray data and the van der Waals atomic radii. r_H values were estimated by assuming the diffusing particles were spherical. ^b Values estimated by introducing the viscosity of nitrobenzene (1.90 cp) in the Stokes–Einstein equation (2).

some participation of the counteranion in the aggregation process could be present. Instead, V_{1c^+}/V_2 shows a wide range of variation, from 7.2 for the lowest concentration up to 40.2 for the highest concentration. It is remarkable that, in the latter situation, an average of about 20 units of $[(\text{Phen})_2\text{Pd}_2(\mu\text{-H})(\mu\text{-CO})]^+$ aggregate in solution. An estimation of the average aggregate volume at different concentrations was obtained by multiplying the ratio V_{1c^+}/V_2 by the volume of the standard **2** (198 \AA^3), calculated starting from X-ray data of similar compounds with the elimination and introduction of suitable ligands, and the van der Waals atomic radii. With the assumption that the diffusing particles are spherical, their average radii were calculated (Table 2). The latter were also estimated by introducing the viscosity of nitrobenzene at 296 K (1.90 cp) in the Stokes–Einstein equation (2) and using corrected self-diffusion coefficients of $1c^+$ ($D_{1c^{+c}}$) that were obtained by multiplying the D_{1c^+}/D_{TMS} ratio by the diffusion coefficients of TMS relative to the 0.43 mM solution. $D_{1c^{+c}}$ coefficients do not have a real meaning, because they represent the diffusion coefficients that $1c^+$ should have at a particular concentration if it were present in a nitrobenzene- d_5 solution with a viscosity equal to that of 0.43 mM solution. On the other hand, these coefficients are very useful for comparing the determined hydrodynamic radii which are not dependent on the solution viscosity. The data are reported in Table 2, and it can be seen that with both methodologies the average radius of the aggregates at the highest concentration is larger than 1 nm. Several cationic moieties of **1c** are involved in the formation of aggregates that slowly diffuse in solution. The compensating counteranions maintain their translational mobility because they probably do not participate greatly in the

(14) Cohen, Y.; Ayalon, A. *Angew. Chem., Int. Ed. Engl.* **1995**, *34*, 816.

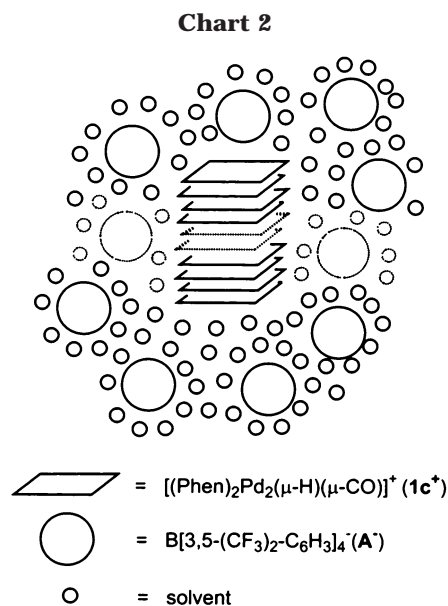


Table 3. Chemical Shift Trends as a Function of the 1c Concentration in Acetone- d_6 at 296 K

C_{1c} (mM)	δ_{H9} (ppm)	δ_{H2} (ppm)	δ_{H7} (ppm)	δ_{H4} (ppm)	δ_{H6} (ppm)	δ_{Pd-H} (ppm)
0.82	9.514	8.670	8.347	8.267	7.633	-13.946
2.12	9.417	8.549	8.261	8.168	7.5383	-14.015
4.36	9.342	8.461	8.200	8.097	7.4705	-14.079
8.89	9.265	8.373	8.138	8.027	7.3983	-14.158
19.80	9.165	8.266	8.066	7.944	7.3134	-14.272
25.13	9.132	8.233	8.044	7.918	7.2877	-14.313
31.98	9.098	8.195	8.019	7.890	7.2596	-14.356
52.41	9.025	8.123	7.970		7.2016	-14.453
67.4	8.977	8.074	7.938	7.799	7.1637	-14.517
87.03	8.922	8.020	7.903	7.759	7.1215	-14.593
110.16	8.858	7.958			7.0708	-14.682
137.34	8.797		7.820	7.668	7.0225	-14.770

formation of the intimate adducts and are surrounded by solvent molecules (Chart 2).

When the trend of V_{1c^+}/V_2 versus C is fitted, it turns out that the V_{1c^+}/V_2 extrapolated value at $C = 0$ is ca. 5: i.e., more than twice the expected value. This indicates that the aggregation of the first two $[(Phen)_2Pd_2(\mu-H)(\mu-CO)]^+$ units occurs even at very low concentrations and that if it were possible to measure V_{1c^+}/V_2 for more dilute solutions, we would observe a discontinuity in the trend with a much more marked decrement as C tends to zero. Furthermore, it suggests that two different types of aggregation processes are present, as also supported by the results obtained when other techniques were used (see below).

1H NMR Chemical Shifts vs. Concentration. In all solvents that we took into account, we observed that the chemical shift values of the resonances belonging to the cationic moiety decreased as the sample concentration increased. As an example, the data relative to acetone- d_6 solutions are reported in Table 3. These trends clearly indicate that one or more cationic moieties closely approach each other and the π -electrons of the phenanthroline ligands afford the well-known shielding effect.¹⁵ From the literature,¹⁶ it is also known that the thermodynamic parameters for the aggregation process

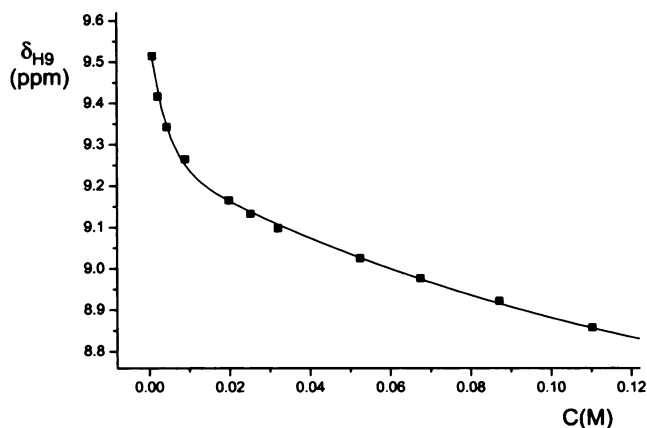


Figure 3. Dependence of the H9 chemical shift on the 1c concentration.

can be deduced from these trends. When we analyzed the δ vs C trends (Figure 3), we realized that there was a discontinuity and the data could not be treated by applying the fitting equations derived from theisodesmic self-association model in which the addition of a molecule to a stack occurs with the identical free energy and equilibrium constant as for the addition of previous molecules. Neither it was possible to use the model in which the enthalpy of addition to a growing stack is constant and successive additions should be increasingly less probable due to the entropic factor.^{16a,17} Although the thermodynamic aggregation parameters were not quantitatively estimated, the trends of the chemical shift values as a function of the concentration afforded another hint about the presence of two energetically distinct processes of aggregation.

UV-Vis Measurements. Other support for the aggregation tendency of $1c^+$ was obtained by the dependence of the absorption spectra on the concentration and temperature. Increasing the concentration or decreasing the temperature of tetrahydrofuran (THF) solutions of $1c$ afforded first the appearance of a band with a maximum around 410 nm followed by a band at 500 nm. The spectral changes in the THF solution absorption spectra as a function of temperature, in the 323–153 K temperature range, are shown in Figure 4. When the temperature is decreased, the intensity of the 410 nm band increases, reaching its maximum value at 213 K. On the other hand, the 500 nm band becomes of appreciable intensity only around 250 K and increases until rigid matrix formation ($T < 164.5$ K). When the sample concentration is increased, an analogous trend is observed, with the 500 nm band becoming detectable when the sample concentration is greater than 5×10^{-3} M. Due to the spectral position and similarity to other organometallic complexes,¹⁸ both bands can be assigned to metal-to-ligand charge transfer (MLCT) transitions. They cannot be intramolecular MLCT transitions, because they only appear when the temperature is decreased or the sample concentration is increased. Consequently, it is reasonable that they are due to two independent aggregation processes. In fact, the intensities of the two bands do not seem to be correlated. Other

(15) Haigh, C. W.; Mallion, R. B. *Prog. Nucl. Magn. Reson. Spectrosc.* **1980**, *13*, 303.

(16) (a) Martin, R. B. *Chem. Rev.* **1996**, *96*, 3043. (b) Mitchell, P. R. *J. Chem. Soc., Dalton Trans.* **1980**, 1079.

(17) Geringer, M.; Gruber, H.; Sterk, H. *J. Phys. Chem.* **1991**, *95*, 2525. Garland, F.; Christian, S. D. *J. Phys. Chem.* **1975**, *79*, 1247.

(18) Arena, G.; Calogero, G.; Campagna, S.; Monsù Scolaro, L.; Ricevuto, V.; Romeo, R. *Inorg. Chem.* **1998**, *37*, 2763–2769.

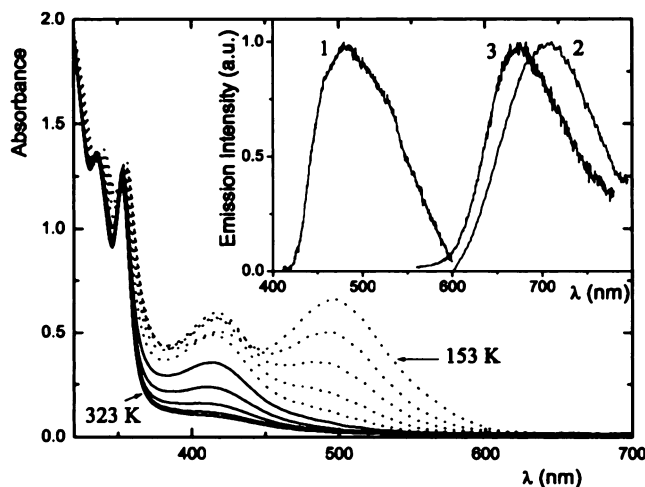


Figure 4. Temperature effects on the absorption spectrum of complex **1c** in THF (2×10^{-4} M). Inset: normalized room-temperature emission spectra of **1c**: (1) a 1×10^{-4} M THF solution excited at 400 nm; (2) a 1×10^{-3} M THF solution excited at 490 nm; (3) powder of **1c** excited at 500 nm (spectrum recorded in reflection).

aggregation evidence could be extracted from the luminescence spectra of complex **1c** in solution as a function of concentration and in the solid state. When a solution of **1c** (1×10^{-4} M) is excited in THF at 400 nm, the emission spectrum 1 is obtained (Insert of Figure 4); spectrum 2 is recorded for a 1×10^{-3} M THF solution excited at 490 nm (almost identical emission spectra were obtained in nitrobenzene solutions). The two different emission spectra support the presence of two distinct molecular assemblies in solution. Furthermore, when a sample of **1c** powder was excited at 500 nm and the reflected emission was collected, spectrum 3 was obtained, which is similar to spectrum 2 obtained in solution by exciting at 490 nm. This indicates that, between the two types of assemblies, the one showing spectrum 2 is more extended and better resembles the solid state. The slight red shift of the maximum of the solution emission spectrum compared with the solid sample (spectra 2 and 3) could be assigned to the stabilization of the excited state, responsible for the emission, due to the polar solvent.

Mass Measurements. Electrospray ionization mass spectrometry (ESIMS) has been widely used for the characterization of nonvolatile high molecular weight compounds and has been applied successfully to the study of self-assembled polynuclear complexes.¹⁹ ESIMS allowed us to identify the various species present in solution.

The positive ion ESI mass spectrum of the complexes present in methanol solution is shown in Figure 5. The spectrum is characterized by an intense peak corresponding to the dinuclear palladium complex and by several weak peaks corresponding to high molecular weight tri- and tetranuclear palladium complexes. The compositions of some ions were confirmed by comparing the theoretical and experimental cluster ions and by MS/MS experiments in which the loss of one or two palladium atoms was observed.

The sample was also analyzed by FAB (fast atom bombardment).²⁰ Although this method of ionization provides a wider extent of fragmentation, we observed a very similar mass spectrum for the high molecular weight species, which confirms the stability of polynuclear aggregates and should exclude the fortuitousness of their observation.

Conclusions

The cationic moiety of $[(\text{Phen})_2\text{Pd}_2(\mu\text{-H})(\mu\text{-CO})]\text{BAR}_4^{\text{F}}$ (**1c**⁺) has a remarkable tendency to form aggregates in solution. Depending on the solution concentration, from 2 up to 20 units of **1c**⁺ form a stack, while its counteranion does not participate in the aggregation process. All the techniques used indicate that two different aggregation processes are active which have completely different energies. The most energetic pathway is responsible for the formation of a dimeric species that is always detectable even at the lowest concentrations with both NMR (0.43 mM) and UV-vis (0.10 mM) measurements. In addition, peaks coming from the fragmentation of the $[(\text{Phen})_2\text{Pd}_2(\mu\text{-H})(\mu\text{-CO})]_2^{2+}$ dimer are observed in the FAB mass spectra. Although X-ray studies (closest interionic Pd–Pd distance 3.23 Å) and theoretical calculations on the analogous complex bearing a Bipy instead of a Phen ligand indicate that π -stacking should have a noncovalent nature,⁹ we suggest that a coordinative contribution should be taken into account for the aggregation of the first two **1c**⁺ moieties. This could lead to the formation of tetrapalladate clusters analogous to those reported by Moiseev et al.²¹ At higher concentration values the least energetic aggregation pathway is active and the aggregation proceeds up to precipitation, without reaching a *plateau*, with the formation of noncovalent adducts in solution having a mean maximum hydrodynamic radius of 11–12 Å.

Experimental Section

Reactions were carried out in a dried apparatus under a dry inert atmosphere of nitrogen using standard Schlenk techniques. One- and two-dimensional ¹H, ¹³C, ³¹P, and ¹⁹F NMR spectra were measured on Bruker DPX 200 and DRX 400 spectrometers. Referencing is relative to TMS (¹H and ¹³C) and CCl₃F (¹⁹F). Two-dimensional ¹H-NOESY and ¹⁹F-¹H-HOESY spectra were recorded with a mixing time of 500–800 ms. The ¹H-¹³C CPMAS{¹H} NMR spectrum was recorded with a Varian Inova 400 MHz spectrometer with a spinning rate of 8.5 kHz.

Synthesis of Complexes 1a–c. Pd(1,10-phenanthroline)-(CH₃COO)₂ (510 mg, 1.25 mmol) and CH₃COOH (0.750 g, 1.25 mmol) were dissolved in a mixture of toluene (15 mL) and 1-butanol (35 mL). After the addition of 50 mL of water, the resulting biphasic system was stirred under carbon monoxide for 2 h at 25 °C. The solution was filtered and vacuum-dried, affording 480 mg of complex **1a** as a red powder. Complex **1b** was prepared by suspending **1a** in methanol in the presence of a large excess of NH₄PF₆. NH₄CH₃COO formed in solution, and after filtration and washing with methanol a quantitative

(20) Barber, M.; Bordoli, R. S.; Sedgwick, R. D.; Tyler, A. N. *J. Chem. Soc., Chem. Commun.* **1981**, 293, 270. Barber, M.; Bordoli, R. S.; Elliott, G. J.; Sedgwick, R. D.; Tyler, A. N. *Anal. Chem.* **1982**, 54, 645A.

(21) Moiseev, I. I. *Pure Appl. Chem.* **1989**, 61, 1755–1762. Moiseev, I. I.; Vargaftik, M. N. *New J. Chem.* **1998**, 1217–1227.

(22) Tyrrell, H. J. W.; Harris, K. R. *Diffusion in Liquids*; Butterworths: London, 1984.

(19) Bonchio, M.; Licini, G.; Modena, G.; Moro, S.; Bortolini, O.; Traldi, P.; Nugent, W. A. *Chem. Commun.* **1997**, 870. Hopfgartner, G.; Piguët, C.; Henion, J. D. *J. Am. Mass. Spectrom.* **1994**, 5, 748.

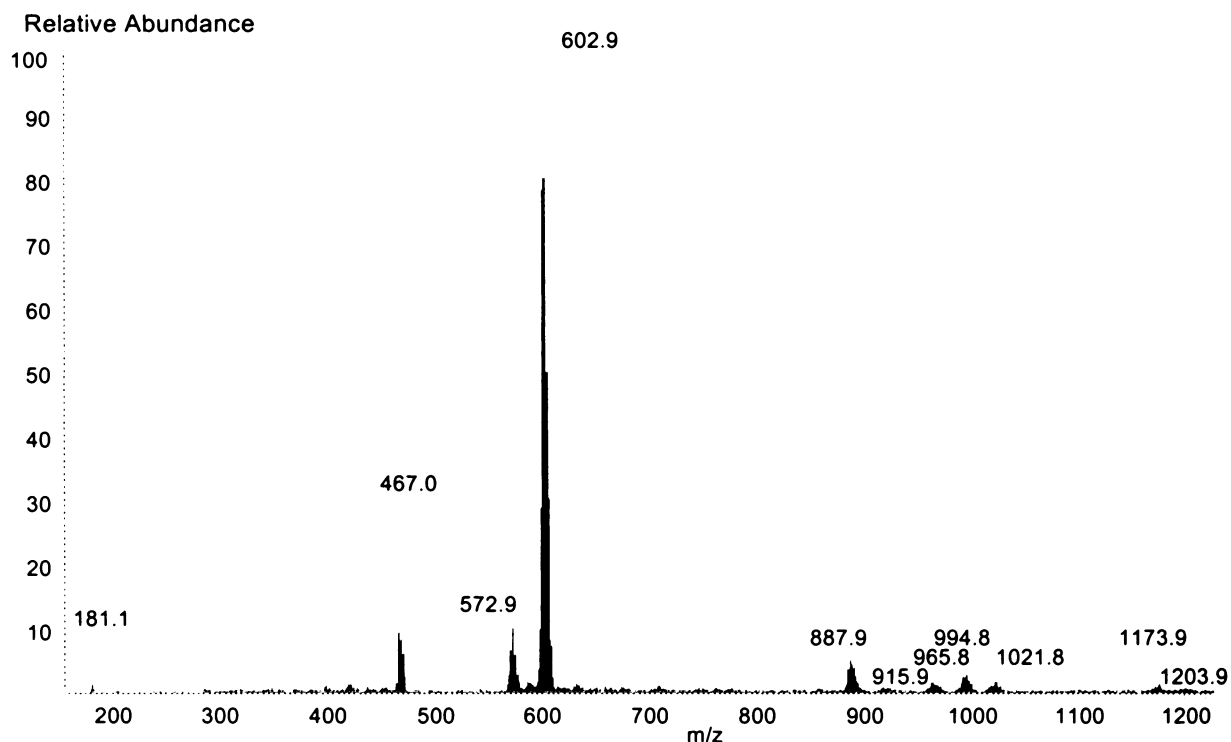


Figure 5. Positive ion ESI mass spectrum of the complex **1c** in methanol solution (m/z , molecular composition): 181.1, [PhenH]⁺; 467.0, [PdPhen₂H]⁺; 572.9, [Pd₂Phen₂ - H]⁺; 602.9, [Pd₂Phen₂COH]⁺; 887.9, [Pd₃Phen₃CO]⁺; 915.9, [Pd₃Phen₃CO₂]⁺; 965.8, [Pd₄Phen₃]⁺; 994.8, [Pd₄Phen₃COH]⁺; 1021.8, [Pd₄Phen₃(CO)₂]⁺; 1173.9, [Pd₄Phen₄CO - H]⁺; 1203.9, [Pd₄Phen₄(CO)₂H₂]⁺.

yield of solid **1b** was obtained. Complex **1c** was prepared by suspending **1a** in methanol followed by the addition of an equimolar quantity of NaBARF₄, which afforded a clean red solution, and precipitation with water. The solid obtained from filtration was washed with water and dried under vacuum. Characterization data for **1c** are as follows. Anal. Found: C, 46.98; H, 2.01, N, 3.79. Calcd for C₅₇H₂₉BF₂₄N₄OPd₂: C, 46.72; H, 1.99; N, 3.82. ¹H NMR (CD₃COCD₃, 298 K, 87.03 mM): δ 8.92 (dd, ³J_{HH} = 4.4, ⁴J_{HH} = 1.4 Hz, H9), 8.02 (dd, ³J_{HH} = 4.4, ⁴J_{HH} = 1.4 Hz, H2), 7.89 (dd, ³J_{HH} = 7.8, ⁴J_{HH} = 1.4 Hz, H7), 7.86 (m, *o*H-BARF₄⁻), 7.75 (dd, ³J_{HH} = 7.8, ⁴J_{HH} = 1.4 Hz, H4), 7.72 (m, *p*-H BARF₄⁻), 7.38 (dd, ³J_{HH} = 7.8, ⁴J_{HH} = 4.4 Hz, H8), 7.16 (dd, ³J_{HH} = 7.8, ⁴J_{HH} = 4.4 Hz, H3), 7.13 (d(AB system), ³J_{HH} = 9.7 Hz, H6), 7.09 (d(AB system), ³J_{HH} = 9.7 Hz, H5), -14.6 (s, Pd-H). ¹³C{¹H} NMR (CD₃COCD₃, 298 K): δ 226.2 (s, CO, ²J_{HC} = 0.9 Hz), 162.2 (q, ¹J_{BC} = 49.9 Hz, C_{ipso} BARF₄⁻), 154.3 (s, C9), 146.4 (s, C2), 143.3 (s, C10'), 143.1 (s, C1'), 138.5 (s, C7), 138.2 (s, C4), 135.1 (m, *o*-C BARF₄⁻), 129.5 (qq, ²J_{FC} = 31.6, ³J_{BC} = 2.9 Hz, *m*-C BARF₄⁻), 128.8 (s, C4'), 128.6 (s, C6'), 126.8 (s, C6), 126.6 (s, C5), 125.3 (s, C8), 124.9 (s, C3), 124.9 (q, ¹J_{FC} = 271.8 Hz, CF₃), 118.0 (m, *p*-C BARF₄⁻). ¹⁹F NMR (CD₃COCD₃, 298 K): δ -63.56 (s, CF₃).

PGSE Measurements. All the measurements were performed on a Bruker AVANCE DRX 400 spectrometer equipped with a GREAT 1/10 gradient unit and a QNP probe with a Z-gradient coil, at 296 K without spinning. The shape of the gradients was rectangular, their duration (δ) was 5 ms, and their strength (G) was varied during the experiments. All the spectra were acquired using 32K points, a spectral width of 12 000 Hz, and a total recycle time of 7 s and were processed with a line broadening of 1.5 Hz. The semilogarithmic plots of $\ln(I/I_0)$ vs G^2 were fitted using a standard linear regression algorithm obtaining an R factor always better than 0.99. Different values of Δ , nt (number of transients), and numbers of different gradient strengths (G) were used for different samples. For the measurements performed using **2** as an internal standard, the nt values were always very high (1024) due to the very low constant concentration of **2**; the Δ values

were set at 106 ms and the number of gradient amplitudes was chosen to have a total time, for each concentration, of less than 12 h (with the exception of the sample having the lowest **1c** concentration (0.43 mmol), for which nt was set at 2048 and the total time was ca. 24 h, using six different gradient strengths). For the measurements performed using TMS as an internal standard, the nt values were changed from 512 to 192 with increasing concentration, while the Δ values were set at 136 ms.

UV-Vis Measurements. The absorption spectra were recorded on a Perkin-Elmer Lambda 800 UV-visible spectrophotometer; light path silica cells were alternatively used in order to obtain corrected spectra of solutions with different optical densities: 10, 1, and 0.1 mm. The emission spectra were recorded on a Spex Fluorolog 2 fluorimeter. An Oxford Instruments cryostat was used for the temperature control.

Mass Measurements. The ESI-MS experiments were performed on a Finnigan LCQ mass spectrometer equipped with an ESI source and a syringe pump. Operating conditions of the ESI source were as follows: spray voltage, 5 kV; capillary voltage, 17 V; heat capillary temperature, 210 °C; tube lens offset voltage, 10 V; sheath gas (N₂), 50 units (roughly 1.25 L/min). The sample dissolved in MeOH was infused via a syringe pump at a flow rate of 2 μ L/min. The instrument was operated in the positive ion mode and scanned from m/z 150 to 2000. The excitation time for CID was 30 ms.

Mass spectra in FAB-MS were obtained using a Finnigan MAT 8400 double-focusing reverse-geometry instrument controlled by a Maspec data system for Windows. The sample was dissolved in a 3-nitrobenzyl alcohol matrix and was deposited on a stainless steel target on the probe into the ion source and subjected to bombardment with xenon accelerated at 8 keV by an M-Scan atom gun operating at 1 mA. The instrument was operated in the positive ion mode and scanned from m/z 150 to 2000.

Selected MS/MS spectra and isotopic distribution are as follows. **603**, [Pd₂Phen₂COH]⁺ (m/z (%)): 603 ([Pd₂Phen₂COH]⁺, 30), 573 ([Pd₂Phen₂COH]⁺ - 30, 25), 467 ([Pd₂Phen₂

COH]⁺ – Pd, 100); isotopic distribution (*m/z* (exptl, theory %)) 597 (9, 9), 598 (25, 26), 599 (62, 62), 600 (76, 74), 601 (80, 83), 602 (73, 77), 603 (100, 100), 604 (50, 51), 605 (71, 74), 606 (19, 20), 607 (31, 32). **888**, [Pd₃Phen₃CO]⁺ (*m/z* (%)): 888 ([Pd₃-Phen₃CO]⁺, 100), 860 ([Pd₃Phen₃CO]⁺ – CO, 35), 708 ([Pd₃-Phen₃CO]⁺ – Phen, 70), 603 ([Pd₃Phen₃CO]⁺ – Phen – Pd, 18); isotopic distribution (*m/z* (exptl, theory %)) 882 (9, 9), 883 (19, 21), 884 (41, 40), 885 (79, 60), 886 (81, 75), 887 (91, 93), 888 (100, 99), 889 (94, 100), 890 (77, 89), 891 (84, 89), 892 (49, 55), 893 (53, 59), 894 (30, 27), 895 (28, 27). **966**, [Pd₄Phen₃]⁺ (*m/z* (%)): 966 ([Pd₄Phen₃]⁺, 100), 860 ([Pd₄Phen₃]⁺ – Pd, 15), 786 ([Pd₄Phen₃]⁺ – Phen, 50); isotopic distribution (*m/z* (exptl, theory %)) 958 (10, 6), 959 (25, 14), 960 (38, 25), 961 (54, 40), 962 (67, 55), 963 (80, 72), 964 (88, 87), 965 (81, 94), 966 (100, 100), 967 (71, 93), 968 (75, 90), 969 (61, 73), 970 (65, 66), 971 (40, 43), 972 (26, 40). **994**, (Pd₄Phen₃COH)⁺ (*m/z* (%)): 994 ([Pd₄Phen₃COH]⁺, 60), 964 ([Pd₄Phen₃COH]⁺ – 30, 100); isotopic distribution (*m/z* (exptl, theory %)) 987 (25, 14), 988 (32, 25), 989 (39, 40), 990 (67, 56), 991 (65, 71), 992 (95, 86), 993 (92, 94), 994 (100, 100), 995 (74, 94), 996 (75, 91), 997 (66, 73), 998 (72, 67), 999 (47, 44), 1000 (47, 40), 1001 (17, 20), 1002 (23, 18), 1003 (15, 11).

FAB–MS spectrum (*m/z* (%)): 181.1 ([PhenH]⁺, 100), 286.0 ([PdPhen]⁺, 57%), 466.0 ([Pd₂Phen]⁺, 11%), 602.9 ([Pd₂Phen₂-COH]⁺, 18%), 965.8 ([Pd₄Phen₃]⁺, 2%), 994.8 ([Pd₄Phen₃COH]⁺, 1.3%), 1173.9, ([Pd₄Phen₄CO – H]⁺, 0.6%), 1203.9 ([Pd₄Phen₄-CO₂H₂]⁺, 0.5%).

Acknowledgment. This work was supported by grants from the Ministero dell'Istruzione, dell'Università e della Ricerca (MIUR, Rome, Italy), Programma di Rilevante Interesse Nazionale, Cofinanziamento 2002–2003. We wish to thank Prof. R. Vivani for the X-ray diffractometric measurements on powders and Dr. F. Ziarelli for the CP MAS ¹³C NMR spectra.

Supporting Information Available: Tables giving all the PGSE NMR data and figures giving the related graphics. This material is available free of charge via the Internet at <http://pubs.acs.org>.

OM0209780